Shifty invisibility cloaks

JOHANNES COURTIAL,[1,*] **JAKUB BĚLÍN,**[1,2,3] **MATÚŠ SOBOŇA,**[2] **MAIK LOCHER,**[1] **AND TOMÁŠ TYC**[4]

[1] *School of Physics and Astronomy, College of Science and Engineering, University of Glasgow, Glasgow G12 8QQ, UK*
[2] *CEITEC – Central European Institute of Technology, Brno University of Technology, Purkyňova 656/123, 612 00 Brno, Czech Republic*
[3] *Faculty of Mechanical Engineering, Institute of Physical Engineering, Brno University of Technology, Technická 2896/2, 616 69 Brno, Czech Republic*
[4] *Department of Theoretical Physics and Astrophysics, Faculty of Science, Masaryk University, Kotlářská 2, 61137 Brno, Czech Republic*
[*]Johannes.Courtial@glasgow.ac.uk

Abstract: We recently presented what we believe are new cloaking strategies [Bělín *et al*., Opt. Express **27**, 37327 (2019)], abstracted from the properties of an ideal-lens cloak that exists in theory only. Key to the cloaking strategies is that objects on the cloak's inside are imaged to its outside. In the simplest case, interior objects appear simply shifted, forming a "shifty cloak". Here we connect our work to several previous investigations of shifty cloaks and other shifty devices, designed using standard transformation optics, thereby bringing our cloaking strategies closer to experimental realization. We investigate to the best of our knowledge novel combinations of shifty cloaks, specifically Janus devices and optical wormholes. Finally, we demonstrate an experimental realization of a paraxial shifty cloak.

1. Introduction

Transformation-optics (TO) molds the flow of light according to the eponymous transformation between two coordinate systems. TO devices on their own can be invisible, but at the same time they can create images of objects that make those objects appear distorted or shifted, often to great effect. The original invisibility cloak [1], for example, makes any objects contained inside it appear at a reduced size when seen from the outside. In principle, the size can be reduced to zero, thereby making the interior objects invisible. Other devices appear to rotate objects [2] or shift the position of objects placed inside [3] or behind [4] the device, and many of these effects were achieved experimentally using metamaterials (e.g. [5,6]), manmade structures that derive their properties from their sub-wavelength shape. Ideas from TO have also been applied to other fields, such as acoustics [7], thermodynamics [8], hydrodynamics [9], and seismic waves [10]; in the latter case, the idea of molding the flow of earthquake waves around cities – effectively cloaking the cities – has a particular attraction.

Several years ago, researchers started studying alternative ways of achieving TO effects. Specifically, a number of relatively low-tech (compared to metamaterials) realizations of invisibility cloaks were demonstrated (e.g. [11–13]). Researchers even used technology that was first created several millennia ago – lenses (it is thought that the earliest known lens, the Nimrud lens, was created between 750BC and 710BC [14]) – to build the so-called *Rochester cloak* [15], a paraxial cloak, that is, a cloak that works only when viewed along lines of sight close to the device's optical axis.

In an attempt to generalize the paraxial lens cloak so that it works from *any* direction, a structure of ideal lenses was subsequently constructed, theoretically, that forms an *omnidirectional* TO

device [16]. Specifically, the structure on its own is invisible and can be interpreted as various types of invisibility cloak [17]. One type of invisibility cloak, poetically named *abyss cloak*, works by imaging objects physically located inside the structure to an exterior position, thereby making them appear to an outside observer to be located exterior to the structure. Such an exterior image is expected to be visible only along lines of sight that intersect both the image and the cloak. Along lines of sight that intersect only the image but not the structure, the image cannot be seen and is therefore invisible. Two nested abyss cloaks can be arranged such that objects at certain positions inside the inner abyss cloak cannot be seen along *any* line of sight, forming an omnidirectional *bi-abyss cloak*.

This generalization of the paraxial lens cloak to an omnidirectional ideal-lens cloak was intended to be the first step of the traditional process for designing lens devices, which comprises first designing a structure of ideal lenses with the desired properties, then replacing the ideal lenses with suitable physical lenses. Unfortunately, however, the imaging characteristics of physical lenses are quite different from those of ideal thin lenses when light passes through the lenses at a wide range of angles, which is necessarily the case in the omnidirectional ideal-lens cloak, a device that is specifically intended to work for *all* directions. For this reason it seems at best difficult, at worst impossible, to build a (good-quality) omnidirectional cloak from physical lenses.

For this reason we have now come full circle, back to designing standard TO devices. What we took from the detour via ideal-lens cloaks is the new cloaking strategies used in abyss cloaks and bi-abyss cloaks which use the fact that an interior volume is imaged to an exterior volume.

The standard TO design process is different from that of our ideal-lens TO devices. We designed our ideal-lens cloak by constructing an invisible structure of ideal thin lenses [16,18], and we then investigated the mapping between physical space and virtual space for this structure, starting in Ref. [16] and continuing in Ref. [17]. In contrast, standard TO starts from a mapping between physical space and virtual space (this mapping, or coordinate transformation, between the two spaces, is the "T" in TO) and calculates corresponding material parameters.

The standard TO approach enables us here to design abyss cloaks in which the physical-to-virtual-space mapping is much simpler than that in ideal-lens cloaks; specifically, the devices we consider here map a void inside the devices to the outside by a pure translation. When seen from the outside, any object inside the central void therefore appears shifted but otherwise unchanged, which is why we refer to such devices as shifty abyss cloaks, or simply shifty cloaks. Additionally, our main designs use mappings that are chosen such that the cloaks consist of polyhedral blocks of homogeneous material (see Ref. [19] for a general discussion of such designs, including shifting devices). Several TO devices comprising polyhedral blocks of homogeneous material, including a polyhedral version of the Pendry cloak [12] and polyhedral carpet cloaks [11,20], have been realized experimentally for visible light, and indeed we hope that our polyhedral shifty cloaks which, in the simplest case, comprise only two different types of material blocks, could also be realized experimentally. Our shifty cloaks are closely related – in some cases almost identical to – several previous designs, some of which are shown in Refs [3,19,21–26]. Note that similar devices have even been realized for heat flow [27,28] and magnetic field [29], the latter for applications to wireless energy transfer. All the optical designs were exclusively analyzed wave-optically and – with the notable exception of Ref. [19] and, to some degree, Ref. [25] – in 2D, whereas we analyze ours ray-optically and in 3D. Furthermore, we show a simplified "paraxial" experiment and investigate novel combinations of shifty cloaks, including Janus devices (which appear to be different things when seen from different directions) [30] and optical wormholes (which appear to connect two distant parts of empty space) [31], thereby significantly extending the combinations presented in Ref. [22].

This paper is organized as follows. In section 2, we start by constructing a shifty cloak using standard TO and demonstrating its visual appearance, including its effect as an abyss cloak,

using raytracing simulations. In section 3, we discuss examples of combinations of shifty cloaks, including (omnidirectional) bi-abyss cloaks, Janus devices, and optical wormholes. Section 4 demonstrates an experimental realization of a "paraxial" shifty cloak. This is followed by a discussion of other aspects of this work and conclusions (Sec. 5). The appendices provide details of the construction of our devices and of the raytracing simulations shown, and they present alternative shifty-cloak designs.

2.   Shifty cloak

We want our shifty cloak to have the following properties, generalized from those of the ideal-lens abyss cloak [17]:

1. The shifty cloak on its own is invisible from all directions.

2. The shifty cloak contains an interior void, and any object placed inside this void appears shifted (and unrotated) when seen from any position outside of the cloak. The shift must be large enough that part of the void, or all of it, appears shifted to outside the cloak.

Figure 1(a) shows a diagram of a 2D device with these properties. The outside of the device is square shaped. A central void is empty, the rest of the device is filled with TO material that makes the central void appear shifted when seen from outside of the device. The diagram also shows several objects inside the central void, the objects in the positions to which they appear shifted when seen from outside of the device, and an illustrative light-ray trajectory that passes between two of the objects and their images. The shifted positions of most of the green disk and the blue disk are outside of the device, as required.

Figure 1(b) shows a cylinder-frame model (a schematic in which cylinders indicate the edges of material blocks) of a 3D version of this device, a cubic device with a cubic central void. As in Fig. 1(a), the image also shows three colored spheres inside the central void, and the same spheres shifted to the positions where they appear when seen from outside of the device. Most of the green sphere, and all of the blue sphere, appear shifted to the outside.

Figure 1(c) shows what happens if the cylinder-frame model in Fig. 1(b) is replaced with the polyhedral blocks of homogeneous TO material. It can be seen that the resulting shifty cloak is invisible (in the simulation, the material has been made slightly absorbing so that the cloak's outline can be seen) and that the spheres appear to be shifted as expected. That this is true not only for the viewpoint for which Figs. 1(b) and (c) were calculated can be seen in Figs. 1(d) and (e). The blue, rightmost, sphere appears shifted to a position outside of the cloak and is therefore visible only along lines of sight that intersect both the shifted position and the cloak; for this reason, it is visible in Fig. 1(e), but not in Fig. 1(c). These are the characteristics of an abyss cloak.
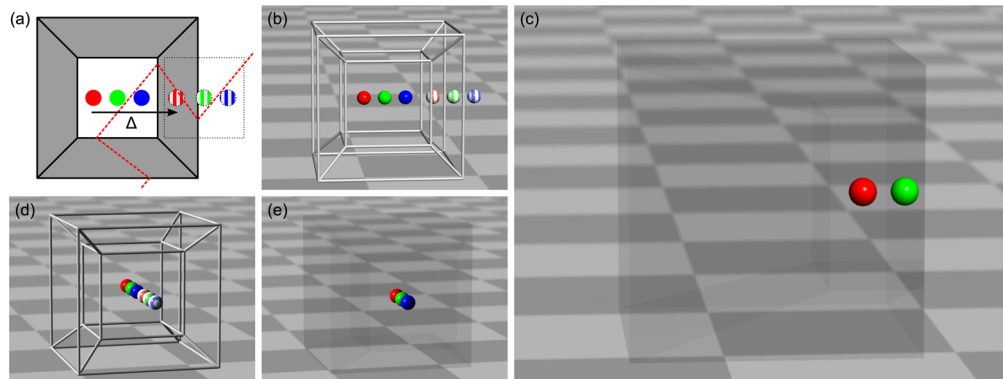
Fig. 1. Cubic shifty cloak. (a) Sketch of the structure and functionality in 2D. The cloak comprises blocks of homogeneous material (gray; black lines show the outline of the blocks). The dashed red line shows a light-ray trajectory through the structure. The square central void contains three disks (solid colors); when seen from the outside, the square, central, void appears shifted to the right (shifted position shown as dotted square) by a distance Δ, and with it the three disks (shifted positions shown striped). (b-e) Raytracing simulations of a 3D shifty cloak (c,e) and its cylinder-frame model (b,d); (b) and (c) are simulated for one camera position, (d,e) for another camera position. In the cloak simulations (c,e), the TO material is slightly absorptive to make it visible. In the cylinder-frame model, each polyhedral block of material is replaced by cylinders marking the block's edges. The cloak contains three colored spheres; in (b,d) striped spheres indicate the shifted positions of these spheres as seen from outside the cloak. Images (b-e) are frames from movies available in Visualization 1 and Visualization 2. Details of the raytracing simulations in this figure and subsequent figures, including links to the source code, runnable binaries, and the parameters used in different simulations, can be found in Supplement 1.

3. Combinations of shifty cloaks: bi-abyss cloaks, Janus devices and optical wormholes

Shifty cloaks can be interesting building blocks for other devices. We demonstrate this here by using them to construct a bi-abyss cloak, a Janus device and an optical wormhole. All of these devices work by creating purely shifted images.

3.1. Bi-abyss cloak

Two nested abyss cloaks can form a bi-abyss cloak, in which the image of certain positions inside the inner abyss cloak cannot be seen from the outside along *any* line of sight [17]. This works as follows. As discussed in the previous section, the image of anything inside an abyss cloak can be visible only along lines of sight that intersect both the image and the cloak, just as any image formed by a lens is visible only along lines of sight that intersect both the image and the lens. The image then appears either in front of the abyss cloak, behind it, or inside it, but never *beside* it. Note, however, that images of interior objects formed *beside* TO devices have been shown to scatter as if they were a real object [32].

   In the absence of the outer abyss cloak, O, the image P′ of any point P inside the inner abyss cloak, I, can therefore be visible only along lines of sight that intersect both P′ and I. If O is added, neither I nor P′ can be seen directly, but only their images due to O, I′ and P″, and P″ can be visible only along lines of sight that intersect P″ and I′. But either of them can be visible only along lines of sight that intersect O. Therefore P″ can be visible only along lines of sight that intersect P″, I′, and O, and if these are arranged such that there is no such line of sight, then P″ is not visible from *any* direction: the bi-abyss cloak is omni-directional.

As abyss cloaks can be realized using shifty cloaks (shifty cloaks *are* abyss cloaks), so can bi-abyss cloaks. Figure 2(a) shows a schematic of an inner shifty cloak, I, nested inside an outer shifty cloak, O, and three colored spheres inside I. The shifts by the two cloaks and the locations of the colored spheres are chosen such that only the image of one of the spheres is visible, along a small range of lines of sight (Fig. 2(b,c)); Fig. 2(a) shows a light ray traveling along one such line of sight. The other spheres are invisible from all directions, and thus cloaked omnidirectionally.
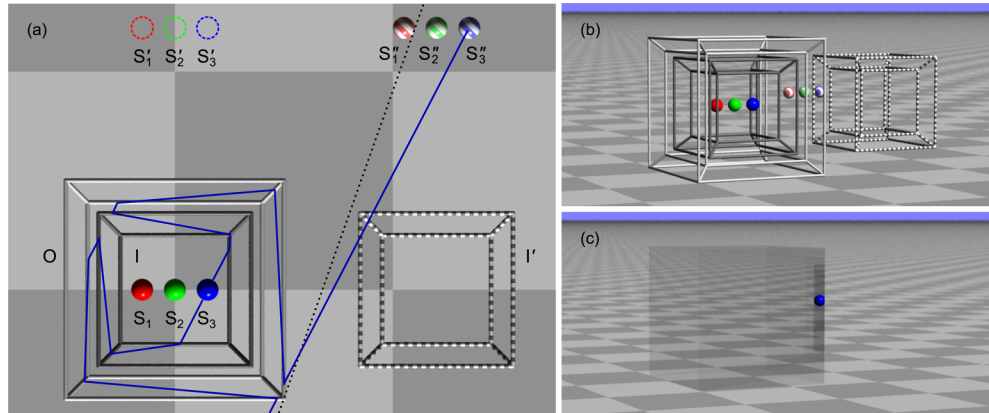

Fig. 2. Bi-abyss cloak based on shifty cloaks. (a) Schematic (top view) of three colored spheres, S_1 to S_3, placed inside the central void inside an inner shifty cloak (dark cylinder-frame model), I, which itself is placed inside the inner void inside an outer shifty cloak (light cylinder-frame model), O. I shifts upwards, creating images S_1' to S_3' (dashed circles) of S_1 to S_3; O, which shifts to the right, re-images these to S_1'' to S_3'', and it images I to I'. The solid blue line represents a ray trajectory that intersects O, I' and S_3'', which means that S_3'' can be visible along the line of sight along which the ray travels outside the cloak. The dotted line is the line that intersects both O and S_1'' and which comes closest to I', but it does not intersect I'. There is therefore no line of sight that intersects O, I' and S_1'', which means S_1'' cannot be visible from *anywhere* outside of O. (b) Like (a), but with the virtual camera placed such that S_3'' is seen along a line of sight that intersects O, I' and S_3''. (c) Like (b), but with the cylinder-frame models of the shifty cloaks replaced by the actual cloaks. As expected, S_3'', the image of the blue sphere, is visible; the others are not. All images are raytracing simulations. The images shown in (b) and (c) are taken from movies available in Visualization 3 and Visualization 4.

3.2. *Janus device*

A Janus device, named after the two-faced Roman god Janus, is a device that looks like different things when seen from different directions. Depending on viewing direction, the original optical Janus device [30] appeared to be either a lens or a (transverse) beam shifter.

A Janus device can be constructed from two shifty cloaks that image their respective interiors into the same volume of space. The directions from which the different images are visible are determined by the requirement that the image of the interior of a particular shifty cloak can be seen only along lines of sight that intersect both the image and the shifty cloak. This is illustrated in Fig. 3(a-d), in which two shifty cloaks create overlapping images of different spheres. The two shifty cloaks were set up as shown in Fig. 3(a), with their shifts selected to image their interiors – two spheres – into the same space. Different light rays that intersect these images can intersect either of the spheres (see Fig. 3(a)) or none. Depending on their position, an observer therefore sees either the image of one sphere (b) or the other (c), or both (d), or none (not shown). Note that

the existence of lines of sight from which both images are visible can be avoided by increasing the distance between the shifty cloaks and the overlapping images they create.
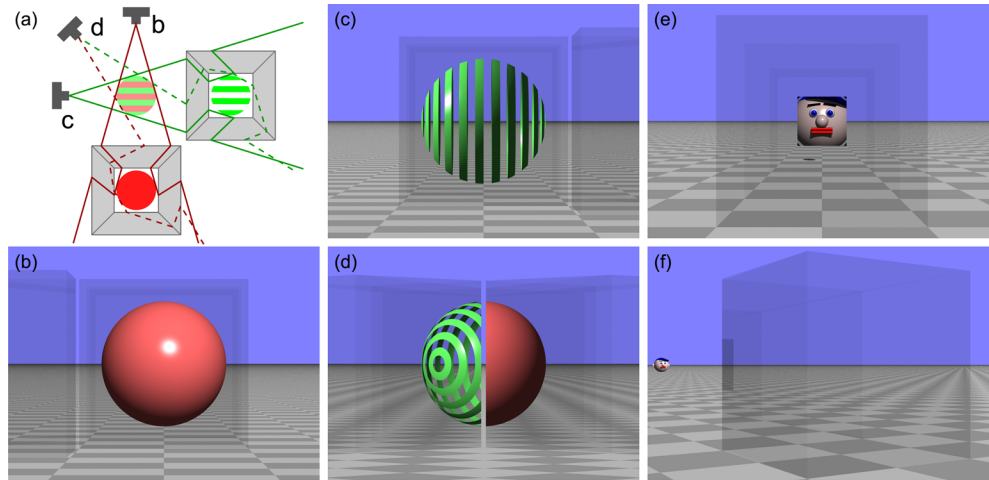

Fig. 3. Janus device (a-d) and optical wormhole (e,f). (a) Top-view diagram of two shifty cloaks, one containing a solid (red) sphere, the other a striped (green) sphere, which image the spheres to the same position (red/green striped sphere). The bottom shifty cloak creates an image that is shifted upwards, the right shifty cloak an image that is shifted to the left. Gray camera silhouettes marked "b", "c", and "d" indicate the camera positions for which the corresponding frames (b-d) are calculated. For each camera, the two rays touching the left and right edges of the images of the spheres are shown. (b,c) Simulated views from camera positions from which the image of the solid sphere (b) and of the striped sphere (c) is visible, but not that of the other sphere, and from a camera position from which the images of *both* spheres are visible (d). (e,f) A shifty cloak that creates an image of a suitable series of lenses, shifted along the optical axis of the lens series, can form an optical wormhole (see Supplement 1 for details of the construction). Objects seen through the wormhole along a line of sight close to the optical axis of the lens series appear closer and therefore magnified (e), whereas from the side the optical wormhole is invisible (and the object, here a head, is seen un-magnified (f)). Frames (b-f) are raytracing simulations in which the shifty cloaks have been made slightly absorbing to make them visible. Frames (b-d) and (e,f) are taken from two movies available in Visualization 5 and Visualization 6.

3.3. Optical wormhole

Shifty cloaks can also be used to create an optical version of "what topologists would call 'a handle' of the multiply-connected space, and what physicists might perhaps be excused for more vividly terming a 'wormhole' " [33]. Reference [31] defines an electromagnetic wormhole as "allowing the passage of waves between possibly distant regions while most of the region of propagation remains invisible."

The original electromagnetic wormhole proposal [31] comprised a waveguide inside a cylindrical cloak that concealed the waveguide when viewed from the side, but which left both ends of the waveguide exposed. In the wavelength for which the device was designed, this structure would then have the appearance of the two ends of the waveguide floating in empty space. In other words, when seen from the side, the wormhole looks like empty space, but when seen along its axis it looks like a waveguide. In this sense, a wormhole is simply a special case of a Janus device.

Our proposal for a wormhole is a Janus device that looks like empty space from the side, but which, when seen along the axis, looks like a device that makes any object seen through it appear closer, but otherwise unchanged, thus creating a "shortcut" between distant parts of space. The device that "shifts" space to make it appear closer could be one of many devices, including a suitable part of a shifty cloak (the parts on opposite sides of a shifty cloak simply shift the view in opposite directions, so that the view through the combination of the two is unshifted) or, like in our simulations, a series of lenses. Details of the wormhole construction can be found in Supplement 1.

Figure 3(e) shows an object (here a head) seen through the wormhole, making the object appear bigger (for comparison, the head is visible directly on the left of Fig. 3(f)), consistent with the object appearing closer. The wormhole is invisible when seen from the side as shown in Fig. 3(f).

4.   Experimental demonstration of a paraxial shifty cloak

Several experiments demonstrating what are essentially shifty cloaks that work only for a limited range of lines of sight have already been published (in addition to several theoretical proposals, such as Refs [34–36]). Reference [37] contains a number of examples, including pairs of thick refractive layers at an angle (see the upper or lower half of the setup shown in Fig. 1 in Ref. [37], which make objects placed between the refractive layers appear shifted downwards or upwards, respectively) and arrangements of planar mirrors such as the one shown in Figs 9-11 in Ref. [37]. Another example is the "terrestrial ray cloak" shown in Fig. 4 of Ref. [13], an arrangement of optical wedge prisms. Here we describe what is essentially one half of this wedge prism arrangement, treating it as a shifty cloak that works for lines of sight close to the observation axis o.

The scheme of the experimental setup is depicted in Fig. 4(a). Four identical wedge prisms, labeled P_1, P_2, P_3 and P_4, are arranged as follows: prism P_2 is oriented opposite to P_1 and offset in a direction perpendicular to the axis of observation, labeled o. The remaining prisms P_3 and P_4 are placed mirror-symmetrically to P_2 and P_1, with respect to a plane $\mathcal{P}$ (a plane perpendicular to the o-axis), whose distance from P_2 can be chosen (in principle) arbitrarily.

Figure 4(b) shows a photo of the experimental setup. The axis of symmetry of the aperture of P_1 forms the o axis. The distance between P_2 and P_3 was chosen arbitrarily, whereas the distances between P_1 and P_2 and consequently between P_3 and P_4 were found such that the images of the apertures P_2, P_3 and P_4 were all centered on the o-axis when seen through P_1 along the o-axis.

Figures 4(c) and (d) show photos of the view along the o axis, demonstrating both the shifting property (c) and the cloaking property (d).
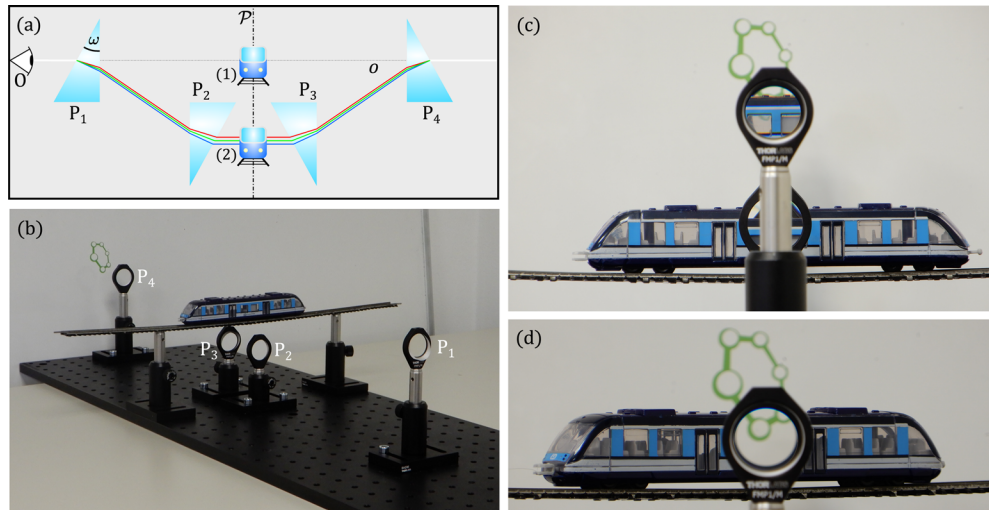
Fig. 4. Paraxial shifty cloak. (a) Diagram of the setup, which comprises four identical wedge prisms, labeled P_1 to P_4, arranged such that the combination first deflects light rays incident along the observation axis o (dotted line) and then restores them to their original trajectory, which means that the combination is invisible when seen along the line of sight o. The symmetric placement of the prisms avoids chromatic aberrations. (b) Photo of the experimental setup, which uses round wedge prisms (aperture diameter 25.4mm, wedge angle $18°9'$). A whiteboard with a logo of CEITEC (Central European Institute of Technology) was used as background scene. (c) A toy train is placed in the trajectory of the deflected light rays (position (2) in (a)). The part of the train that is visible through the aperture of P_1 (and along the observation axis o) appears shifted upwards. (d) If the train is placed across the observation axis o (position (1) in (a)), and nothing obstructs the deflected light rays, the background is visible through P_1 and part of the train appears invisible. See also Visualization 7 and Visualization 8.

5.   Discussion

The cubic shifty cloak is designed to consist of polyhedral blocks of homogeneous material (in Fig. 1(b), the edges of the polyhedral blocks are indicated by cylinders), which is achieved by choosing the mapping between physical space and virtual space to be piecewise affine, specifically such that the mapping between each polyhedral block in physical space and its corresponding polyhedral block in virtual space is affine; details can be found in App. A. The intention behind designing the device in this way is to make it easier to realize experimentally, and indeed a number of TO devices designed in this way have been realized experimentally [11,12,20].

   The cubic device described in Sec. 2 is only one possible realization of the shifty cloak. App. A discusses several other polyhedral devices and App. B describes a spherical device. Like the cubic shifty cloak, our other polyhedral devices are designed to be manufactured from polyhedral blocks of homogeneous materials. In a regular tetrahedral cloak, if the shift is perpendicular to one of the faces, then the material blocks corresponding to the three other faces are all identical, so there are only two different types of material block required.

   This structural simplicity of the regular tetrahedral shifty cloak suggests that it might be easy to realize such a device experimentally. On the other hand, if some part of virtual space reaches to the outside of the cloak, then at least one of the blocks must exhibit negative refraction, and it is hard to realize the required "negative materials" experimentally. Indeed, upon the transformation from physical to virtual space, there is a portion of space where the Jacobian transformation matrix from physical to virtual space (see App. A) has negative determinant; or, equivalently, a

triplet of vectors changes handedness (from left-handed to right-handed or vice versa) upon this transformation. The direction change typical of negative refraction can be spotted in several of the ray trajectories shown in Figs. 1(a), 2(a) and 3(a), specifically in the blocks on the same side of the shifty cloak as the image of the cloak's interior. This requirement for negative refraction, already noted in Ref. [25], makes it hard to realize such a cloak over a wide range of wavelengths and with low loss, and restricts the materials employed to artificial metamaterials. On the other hand, progress in the manufacture of optical metamaterials is rapid and may enable a practical broadband shifty cloak in future. For example, active metamaterials [38] look set to overcome loss issues.

We stress that our shifty cloaks, especially the cubic shifty cloak, are related to other beam-shifting devices [34,35], most closely to those presented in Refs [22–26]. In all cases, the devices comprise slabs of homogeneous materials that shift light on transmission (e.g. [4,39–42]). The shifty devices are invisible combinations of such shifting slabs; slabs on opposite sides shift by the same distance but in opposite directions (see, e.g., [34]).

Our shifty cloaks are also related to the Calcite carpet cloaks described in Refs [11,20], which can be viewed as portions of shifty cloaks. However, these Calcite carpet cloaks work only for one plane of incidence, which makes them effectively two-dimensional. There is a good reason for this, which applies also to our shifty devices comprising polygonal blocks of uniform material: in the 2D case a uniaxial medium such as Calcite is sufficient, while for a full 3D functionality one needs in general a completely anisotropic medium.

A pixellated, ray-optical, version of polyhedral shifty cloaks can, at least in principle, be realized using microstructured sheets called generalized confocal lenslet arrays (GCLAs) [43]. GCLAs have many shortcomings, such as limited field of view. Existing GCLA cloak proposals [44,45] have structures similar to those of the shifty cloaks discussed here, but the cloaking mechanism is very different.

Our paraxial shifty cloak shows that shifty cloaks that work for a small range of lines of sight can be constructed relatively easily. Along those lines of sight for which the cloak works there are imperfections that include image aberrations (because, unlike planar mirrors, wedge prism do not image stigmatically), the image distance being wrong (because the rays take a detour inside the shifty cloak), and dispersion effects. None of these effects are visible in our experimental results (Fig. 4), due to the effects being small for all lines of sight for which the cloak works, but if required the issues of image aberrations and dispersion could easily be avoided by folding the beam path using mirrors instead of prisms.

The feature of all of our combinations of (non-paraxial) shifty cloaks that makes them surprising is that the devices themselves are invisible, which is not the case for combinations of paraxial shifty cloaks. Still, looking for interesting effects in paraxial shifty cloaks combined into paraxial bi-abyss cloaks, Janus devices, or wormholes is a potentially worthwhile task for future research. But the main significance of paraxial (shifty) cloaks is that they allow cloaking to be approached from the direction of very restricted cloaking using a very simple setup, and the primary challenge then becomes lifting the restrictions, in our case increasing the field of view.

One key aspect of shifty cloaks is their cloaking ability, but this is more complicated than at first it appears. As discussed in Sec. 2, any object inside a shifty cloak that is imaged by the cloak to a position outside of the cloak can be seen by an outside observer only along lines of sight that intersect both the image and the cloak. Wave-optically, hiding an object from view is the prevention of scattering from that object, and indeed this is what is found in Ref. [26]. Interestingly, the device analyzed in Ref. [26] prevents scattering of waves incident from *all* directions, which seems to be at odds with the finding that ray-optical cloaking works only along specific lines of sight, and therefore only certain directions. In other setups [22,24,46], the exact opposite happens: the outside image *scatters* light from all directions. The situation becomes more confusing still when considering Ref. [23], which discusses a shifty device placed above a

mirror, in which the cloaking effect depends not on lines of sight or directions, but on the image's position relative to the mirror: if the image created by the shifty device of its interior void is located *below* the mirror, then that image is invisible from all directions. (This is very different from what would happen ray-optically, where the image would be visible along lines of sight that intersect both the cloak and the image.)

6.   Conclusions

We have discussed shifty cloaks, TO devices that appear to shift an interior region of space to the outside. According to our ray-optical analysis, shifty cloaks can make the cloaked object invisible when seen from a limited range of viewing directions, and future work should aim to reconcile our result with the apparently contradictory findings regarding scattering by shifty cloaks. We have also demonstrated that shifty cloaks are remarkably versatile: other TO devices, such as perfect invisibility cloaks, Janus devices or optical wormholes, can in principle be constructed from shifty cloaks. Finally, we have realized a simple paraxial shifty cloak experimentally, using wedge prisms – the shifty-cloak analog of the Rochester cloak [15].

The advantage of shifty cloaks is that they can arguably be built using metamaterials with simpler material properties than those required for standard, "shrink", invisibility cloaks [1,47]; we have shown that shifty cloaks can be built of homogeneous blocks of material and, in the simplest case, there are only two different types of blocks of material included in the device.

Our work provides the missing link between ideal-lens TO (defined in Refs [16–18]) and standard TO [1,48]. Specifically, the cloaking ideas that were developed using ideal-lens TO [17] are simplified and applied to standard TO, resulting in shifty cloaks.

Obvious directions for future work are a further improvement of the paraxial shifty cloak, extending the range of viewing directions, and efforts to realize omnidirectional shifty cloaks experimentally.

Appendix A. Polyhedral shifty TO devices

We design our polyhedral shifty TO devices such that the mapping between physical space and virtual space is piecewise affine, which means that such devices can be realized with piecewise homogeneous blocks of material. Due to the simplicial approximation theorem [49,50], this is always possible if the spaces are divided into simplices (triangles in 2D and tetrahedra in 3D). An example of such a device, namely in the dual tetrahedral device, is shown in Fig. 5(a).

Any affine transformation is a composition of a translation and a linear map. In vector notation, it can be written as

$$\mathbf{x}' = A\mathbf{x} + \mathbf{b}, \tag{1}$$

where $\mathbf{x}$ and $\mathbf{x}'$ are position vectors in virtual and physical spaces, respectively, A is the matrix describing the linear map and $\mathbf{b}$ is the translation vector. Note that in the 3D case, the mapping is specified by 12 parameters: 9 entries of the matrix A plus 3 components of the vector $\mathbf{b}$; these parameters can be uniquely determined if we know physical-space images of four virtual-space points, for example the simplex vertices.

From Eq. (1) we can calculate the Jacobian transformation matrix

$$\Lambda_j^i = \frac{\partial x'^i}{\partial x^j} = A_{ij}, \tag{2}$$

and following the general procedure of transformation optics [51] we find the corresponding material parameters

$$\varepsilon'^{ij} = \mu'^{ij} = |\det \Lambda|^{-1} \Lambda_k^i \Lambda_l^j \delta^{kl} = |\det A|^{-1} A_{ik} A_{jk}, \tag{3}$$

where we have taken into account that the relative permittivity and permeability tensors in virtual space are given by the unit matrix, $\varepsilon^{kl} = \mu^{kl} = \delta^{kl}$.
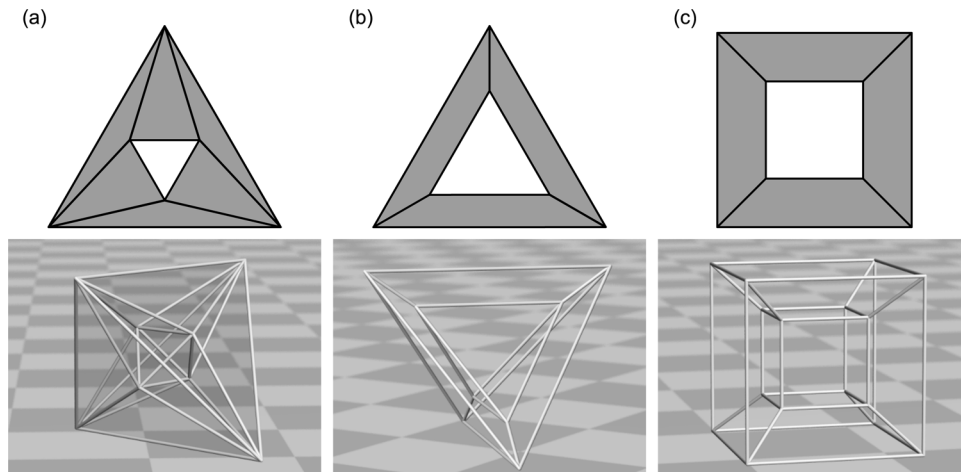
Fig. 5. Physical-space structure of several polygonal cloaks in 2D (top row) and 3D (bottom row). The white regions are filled with vacuum; gray regions indicate a (generally anisotropic) material.

Sometimes, it is possible to design the device such that the affine mappings in neighboring simplices are identical. The corresponding physical-space simplices are then filled with identical material, and so they can be seen as parts of the same polyhedral block of material. Two of our devices, namely the cubic and simple tetrahedral devices shown in Fig. 5(b) and (c), are of this kind. They require relatively few material blocks – 6 in the case of the cubic device (Fig. 5(c)), 4 in the case of the tetrahedral device (Fig. 5(b)) – and if the shift direction is chosen appropriately, the devices can be relatively simple: if the shift direction is chosen in the direction from the centroid to one of the vertices, the tetrahedral device consists of only two different types of block.

As an example of this type, we calculate the material parameters of the shifty cloak shown in Fig. 5(b). Figure 6 shows the physical and virtual spaces for this device. Its physical space consists of two concentric regular tetrahedra of side lengths a and b and four pentahedra squeezed between them. In virtual space, the outer tetrahedron coincides with the one of physical space. The inner tetrahedron is shifted by the distance s in the direction perpendicular to one of its faces, and the four pentahedra are transformed accordingly. Since the inner tetrahedron is just shifted upon the transformation, in physical space it remains empty (i.e., filled with vacuum). As the transformation from physical space to virtual space for the bottom pentahedron reverses direction of one coordinate, the resulting material is negatively refracting. As for the three upper pentahedra, the transformation (1) is the same for all of them, and so are the (anisotropic) permittivity and permeability tensors. One can express the material tensors analytically as functions of a, b and s. However, the formulas are too complicated to be stated here. Therefore we just write down the eigenvalues of the relative permittivity tensor for a particular example of $b = a/2$ and $s = (2/3)^{3/2}a$, which corresponds to the upper tip of the inner tetrahedron of virtual space just touching the bottom face of the outer tetrahedron. The numerical eigenvalues for the bottom pentahedron are in this case $-3, -1/3$ and $-1/3$, and for the upper three pentahedra we get eigenvalues 13.92, 1/3 and 0.0718.
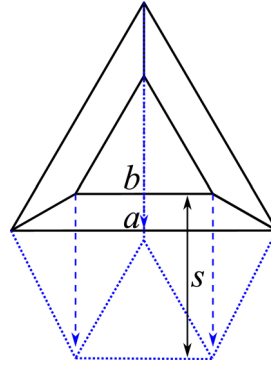
Fig. 6. Scheme of the tetrahedral shifty cloak. Physical space consists of two concentric regular tetrahedra with sides a and b (solid-black), and four pentahedra between them. To get the mapping into virtual space (dotted-blue), we shift the inner tetrahedron by a distance s in the direction of the blue dashed arrows.

Appendix B. Other configurations for shifty TO devices

Here we design a simple shifty TO device using standard TO techniques. For simplicity, we discuss the device in 2D; the generalization to 3D is obvious.

Figure 7(a) shows a "smooth top-hat function" $s(r)$, defined such that

$$s(r) = \begin{cases} 1 & : & r \leq r_1, \\ p((r - r_1)/(r_0 - r_1)) & : & r_1 < r \leq r_0, \\ 0 & : & r > r_0, \end{cases} \tag{4}$$

where $r_1 < r_0$ and

$$p(x) = 2x^3 - 3x^2 + 1 \tag{5}$$

is a polynomial with the properties $p(0) = 1$, $p(1) = 0$, $p'(0) = p'(1) = 0$. Using this smooth top-hat function, we can then easily construct a mapping

$$\begin{pmatrix} x' \\ y' \end{pmatrix} = \begin{pmatrix} x + s\left(\sqrt{x^2 + y^2}\right)\Delta x \\ y + s\left(\sqrt{x^2 + y^2}\right)\Delta y \end{pmatrix} \tag{6}$$

with the properties that

1. inside the smaller circle of radius r_1, the mapping is a uniform shift by $(\Delta x, \Delta y)$;

2. outside the larger circle of radius r_0, the mapping is the identity map;

3. between the two circles, the mapping smoothly interpolates between the other two mappings.

Figure 7(b) shows an example of the effect of this map on a rectangular grid.

If this map is chosen as the "transformation" from physical space to virtual space, and a device constructed following the standard TO "recipe" (which can be found e.g. in Ref. [52]), then the resulting material structure is confined inside the outer circle of radius r_0 and empty inside the inner circle of radius r_1. In the space between the circles, the material structure is inhomogeneous and anisotropic. It is index matched at both circles, meaning that there are no reflections. When seen from outside the outer circle, the material structure makes any object inside the inner circle
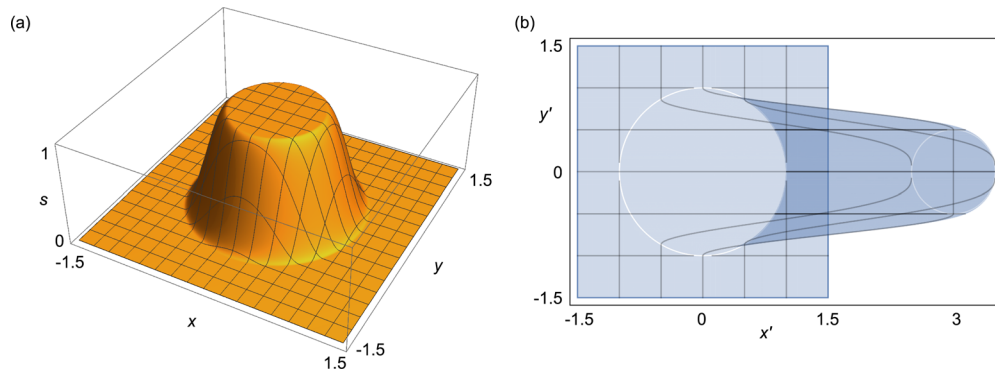
(a)

(b)

Fig. 7. (a) Smooth top-hat function, $s(r) = s(\sqrt{x^2 + y^2})$, plotted for $r_1 = 0.5$, $r_0 = 1$ over a range $-1.5 \leq x, y \leq 1.5$. (b) Rectangular grid in physical space covering the range $-1.5 \leq x, y \leq 1.5$, mapped into virtual space using the smooth top-hat function in (a) with a shift $(\Delta x, \Delta y) = (3, 0)$.
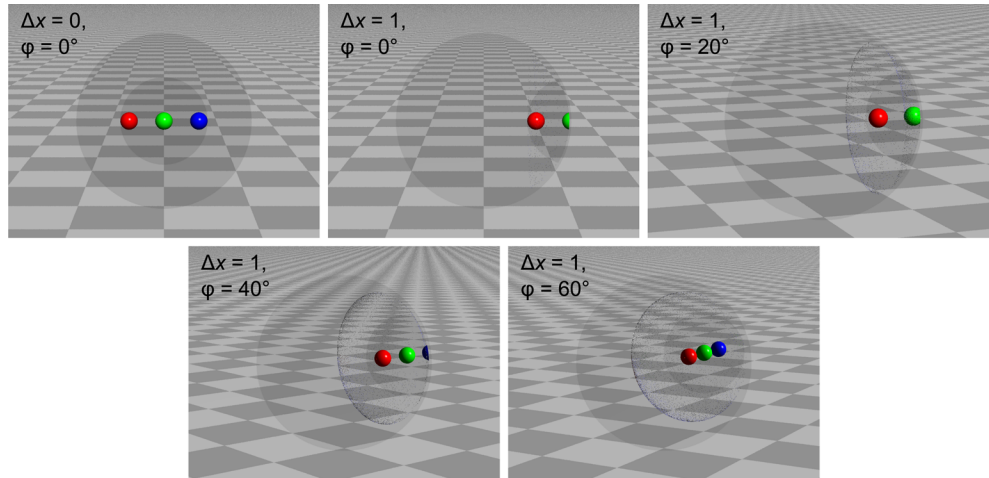

$\Delta x = 0$, $\varphi = 0°$

$\Delta x = 1$, $\varphi = 0°$

$\Delta x = 1$, $\varphi = 20°$

$\Delta x = 1$, $\varphi = 40°$

$\Delta x = 1$, $\varphi = 60°$

Fig. 8. Raytracing simulations of a spherical shifty cloak. Three spheres were placed inside a spherical shifty cloak, calculated for $r_1 = 0.5$ and $r_1 = 1$, that translates the inner spherical region by Δx in the x direction. To illustrate the setup, the top left image was calculated for $\Delta x = 0$, which means the image simply shows physical space. The remaining images were calculated for $\Delta x = 1$, from different viewing angles. The virtual camera is placed such that the center of the device is viewed along a direction at an angle $\varphi + 90°$ relative to the shift direction. The black dots visible in the frames for $\varphi = 20°$, $\varphi = 40°$ and $\varphi = 60°$ are numerical artifacts. The images calculated for $\Delta x = 1$ are frames taken from a movie available in Visualization 9.

appear shifted by $(\Delta x, \Delta y)$ and any object outside the outer circle unshifted (and undistorted in any other way).

Figure 8 shows raytracing simulations of the 3D version of such a material structure, confirming its effect as a "shifty cloak".

Disclosures. The authors declare that there are no conflicts of interest related to this article.

Data availability. The data that were created in this research are in the form of calculations, raytracing simulations and experimental photos. Data not presented in this paper may be obtained from the authors upon reasonable request.

The Supplement 1 contains links to the source code and executable binaries for the raytracing software (an extended version of *Dr TIM* [53]) used to create the raytracing simulations in this paper, plus details on the parameters used.

Supplemental document. See Supplement 1 for supporting content.

References

1. J. B. Pendry, D. Schurig, and D. R. Smith, "Controlling electromagnetic fields," Science **312**(5781), 1780–1782 (2006).
2. H. Chen and C. T. Chan, "Transformation media that rotate electromagnetic fields," Appl. Phys. Lett. **90**(24), 241105 (2007).
3. H. A. Madni, B. Zheng, M. Akhtar, *et al.*, "A bi-functional illusion device based on transformation optics," J. Opt. **21**(3), 035104 (2019).
4. M. Rahm, S. A. Cummer, D. Schurig, *et al.*, "Optical design of reflectionless complex media by finite embedded coordinate transformations," Phys. Rev. Lett. **100**(6), 063903 (2008).
5. D. Schurig, J. J. Mock, B. J. Justice, *et al.*, "Metamaterial Electromagnetic Cloak at Microwave Frequencies," Science **314**(5801), 977–980 (2006).
6. H. Chen, B. Hou, S. Chen, *et al.*, "Design and experimental realization of a broadband transformation media field rotator at microwave frequencies," Phys. Rev. Lett. **102**(18), 183903 (2009).
7. H. Chen and C. T. Chan, "Acoustic cloaking in three dimensions using acoustic metamaterials," Appl. Phys. Lett. **91**(18), 183518 (2007).
8. R. Schittny, M. Kadic, S. Guenneau, *et al.*, "Experiments on transformation thermodynamics: Molding the flow of heat," Phys. Rev. Lett. **110**(19), 195901 (2013).
9. J. Park, J. R. Youn, and Y. S. Song, "Hydrodynamic metamaterial cloak for drag-free flow," Phys. Rev. Lett. **123**(7), 074502 (2019).
10. S. Brûlé, E. H. Javelaud, S. Enoch, *et al.*, "Experiments on seismic metamaterials: Molding surface waves," Phys. Rev. Lett. **112**(13), 133901 (2014).
11. B. Zhang, Y. Luo, X. Liu, *et al.*, "Macroscopic invisibility cloak for visible light," Phys. Rev. Lett. **106**(3), 033901 (2011).
12. H. Chen and B. Zheng, "Broadband polygonal invisibility cloak for visible light," Sci. Rep. **2**(1), 255 (2012).
13. H. Chen, B. Zheng, L. Shen, *et al.*, "Ray-optics cloaking devices for large objects in incoherent natural light," Nat. Commun. **4**(1), 2652 (2013).
14. British Museum The, "Collection online. The Nimrud Lens / The Layard Lens," http://www.britishmuseum.org/research/collection_online/collection_object_details.aspx?objectId=369215&partId=1.
15. J. S. Choi and J. C. Howell, "Paraxial ray optics cloaking," Opt. Express **22**(24), 29465–29478 (2014).
16. J. Courtial, T. Tyc, J. Bělín, *et al.*, "Ray-optical transformation optics with ideal thin lenses makes omnidirectional lenses," Opt. Express **26**(14), 17872–17888 (2018).
17. J. Bělín, T. Tyc, M. Grunwald, *et al.*, "Ideal-lens cloaks and new cloaking strategies," Opt. Express **27**(26), 37327–37336 (2019).
18. T. Tyc, J. Bělín, S. Oxburgh, *et al.*, "Combinations of generalized lenses that satisfy the edge-imaging condition of transformation optics," J. Opt. Soc. Am. A **37**(2), 305–315 (2020).
19. C. Yang, M. Huang, J. Yang, *et al.*, "General design of 3D piecewise homogeneous illusion devices with arbitrary shapes," J. Appl. Phys. **128**(1), 014503 (2020).
20. X. Chen, Y. Luo, J. Zhang, *et al.*, "Macroscopic invisibility cloaking of visible light," Nat. Commun. **2**(1), 176 (2011).
21. W. Li, J. Guan, Z. Sun, *et al.*, "Shifting cloaks constructed with homogeneous materials," Comput. Mater. Sci. **50**(2), 607–611 (2010).
22. X. Zang and C. Jiang, "Overlapped optics, illusion optics, and an external cloak based on shifting media," J. Opt. Soc. Am. B **28**(8), 1994–2000 (2011).
23. X. Zang, B. Cai, and Y. Zhu, "Shifting media for carpet cloaks, antiobject independent illusion optics, and a restoring device," Appl. Opt. **52**(9), 1832–1837 (2013).
24. Y. Du, X. Zang, C. Shi, *et al.*, "Shifting media induced super-resolution imaging," J. Opt. **17**(2), 025606 (2015).
25. F. Sun, Y. Liu, and S. He, "True dynamic imaging and image composition by the optical translational projector," J. Opt. **18**(4), 044012 (2016).
26. C. Yang, M. Huang, J. Yang, *et al.*, "Target illusion by shifting a distance," Opt. Express **26**(19), 24280–24293 (2018).
27. Y. Liu, F. Sun, and S. He, "Novel thermal lens for remote heating/cooling designed with transformation optics," Opt. Express **24**(6), 5683–5692 (2016).
28. Y. Liu, K. Chao, F. Sun, *et al.*, "Active thermal metasurfaces for remote heating/cooling by mimicking negative thermal conductivity," Adv. Mater. **35**(29), 2210981 (2023).

29. S. Li, F. Sun, D. An, *et al.*, "Increasing efficiency of a wireless energy transfer system by spatial translational transformation," IEEE Trans. Power Electron. **33**(4), 3325–3332 (2018).

30. T. Zentgraf, J. Valentine, N. Tapia, *et al.*, "An optical "janus" device for integrated photonics," Adv. Mater. **22**(23), 2561–2564 (2010).

31. A. Greenleaf, Y. Kurylev, M. Lassas, *et al.*, "Electromagnetic wormholes and virtual magnetic monopoles from metamaterials," Phys. Rev. Lett. **99**(18), 183901 (2007).

32. Y. Xu, S. Du, L. Gao, *et al.*, "Overlapped illusion optics: a perfect lens brings a brighter feature," New J. Phys. **13**(2), 023010 (2011).

33. C. W. Misner and J. A. Wheeler, "Classical physics as geometry," Ann. Phys. **2**, 525–603 (1957).

34. M. Y. Wang, J. J. Zhang, H. Chen, *et al.*, "Design and application of a beam shifter by transformation media," Prog. Electromagn. Res. **83**, 147–155 (2008).

35. G. X. Yu, W. X. Jiang, and T. J. Cui, "Invisible slab cloaks via embedded optical transformation," Appl. Phys. Lett. **94**(4), 041904 (2009).

36. S. Xi, H. Chen, B.-I. Wu, *et al.*, "One-directional perfect cloak created with homogeneous material," IEEE Microw. Wireless Compon. Lett. **19**(3), 131–133 (2009).

37. J. C. Howell and J. B. Howell, "Simple, broadband, optical spatial cloaking of very large objects," arXiv, arXiv:1306.0863 (2013).

38. S. Xiao, T. Wang, T. Liu, *et al.*, "Active metamaterials and metadevices: a review," J. Phys. D: Appl. Phys. **53**(50), 503002 (2020).

39. I. Gallina, G. Castaldi, V. Galdi, *et al.*, "General class of metamaterial transformation slabs," Phys. Rev. B **81**(12), 125124 (2010).

40. G. Gok and A. Grbic, "A beam-shifting slab implemented using printed, tensor TL metamaterials," *2012 IEEE/MTT-S International Microwave Symposium Digest (Montreal, QC, Canada)* pp. 1–3 (2012).

41. M. Salmasi, M. Okoniewski, and M. E. Potter, "A broadband metamaterial based beam-shifter," *2016 IEEE International Symposium on Antennas and Propagation (APSURSI)* (2016).

42. O. Reshef, M. P. DelMastro, K. K. M. Bearne, *et al.*, "An optic to replace space and its application towards ultra-thin imaging systems," Nat. Commun. **12**(1), 3512 (2021).

43. A. C. Hamilton and J. Courtial, "Generalized refraction using lenslet arrays," J. Opt. A: Pure Appl. Opt. **11**(6), 065502 (2009).

44. S. Oxburgh, C. D. White, G. Antoniou, *et al.*, "Transformation optics with windows," Proc. SPIE **9193**, 91931E (2014).

45. T. Tyc, S. Oxburgh, E. N. Cowie, *et al.*, "Omni-directional transformation-optics cloak made from lenses and glenses," J. Opt. Soc. Am. A **33**(6), 1032–1040 (2016).

46. Y. Luo, J. J. Zhang, H. Chen, *et al.*, "Wave and ray analysis of a type of cloak exhibiting magnified and shifted scattering effect," Prog. Electromagn. Res. **95**, 167–178 (2009).

47. U. Leonhardt and T. Tyc, "Broadband Invisibility by Non-Euclidean Cloaking," Science **323**(5910), 110–112 (2009).

48. U. Leonhardt, "Optical conformal mapping," Science **312**(5781), 1777–1780 (2006).

49. P. J. Hilton and S. Wylie, *Homology Theory: An Introduction to Algebraic Topology* (Cambridge University Press, 1960), chap. 1.8, p. 37.

50. Wikipedia, "Simplicial approximation theorem," https://en.wikipedia.org/wiki/Simplicial_approximation_theorem.

51. D. Schurig, J. B. Pendry, and D. R. Smith, "Calculation of material properties and ray tracing in transformation media," Opt. Express **14**(21), 9794–9804 (2006).

52. U. Leonhardt and T. Philbin, *Geometry and Light. The Science of Invisibility* (Dover Publications, Inc., 2010).

53. S. Oxburgh, T. Tyc, and J. Courtial, "Dr TIM: Ray-tracer TIM, with additional specialist scientific capabilities," Comp. Phys. Commun. **185**(3), 1027–1037 (2014).